Research Square

Preprints are preliminary reports that have not undergone peer review.
They should not be considered conclusive, used to inform clinical practice,
or referenced by the media as validated information.

How do regional blood flow rates measured by arterial Doppler vary during hemorrhagic shock? An experimental study in anesthetized piglets

Colin Azria

colinazria@gmail.com

IMAGINE, University of Montpellier, Montpellier University Hospital

Céline Occelli

Centre Hospitalier Universitaire de Nice

Edwin Bodet

Timone University Hospital, APHM

Thomas Sanchez

IMAGINE, University of Montpellier, Montpellier University Hospital

Thibaut Markarian

Timone University Hospital, APHM

Florian Ajavon

IMAGINE, Montpellier University, Nîmes University Hospital

Marylène Bacle

Montpellier University

Xavier Bobbia

IMAGINE, University of Montpellier, Montpellier University Hospital

Fabien Coisy

IMAGINE, Montpellier University, Nîmes University Hospital

Article

Keywords: Regional Blood flow, Doppler, Piglets, Time-averaged mean velocity

Posted Date: November 2nd, 2026

DOI: https://doi.org/10.21203/rs.3.rs-10897050/v1

License: This work is licensed under a Creative Commons Attribution 4.0 International License.
Read Full License

Additional Declarations: Competing interest reported. CA declares a conflict of interest for this study with Agence régionale de santé Occitanie, as he received a one-year research fellowship funded by Agence régionale de santé Occitanie. Other authors declare that they have no competing interests.

Abstract

Hemorrhagic shock induces compensatory vasoconstriction that may affect arterial territories differently. Regional blood flow (RBF) can be assessed using Doppler ultrasound with the time-averaged mean velocity (TAMV). The primary objective was to describe changes in RBF among the carotid, femoral, superior mesenteric and renal arterial territories across blood depletion during controlled hemorrhagic shock in anesthetized piglets.

Anesthetized and mechanically ventilated piglets underwent controlled blood withdrawal at 2 $mL \cdot kg^{-1} \cdot min^{-1}$ until a mean arterial pressure of 40 mmHg was reached. At baseline and after each 5-$mL \cdot kg^{-1}$ depletion step, VTI was measured in the carotid, femoral, superior mesenteric and renal arteries. TAMV was calculated as VTI × HR / 60 and normalized to each animal's baseline value. TAMV was analyzed using linear mixed-effects models with a subject-specific random intercept. Fixed effects were assessed using type III analysis of variance and reported as *F* statistics with Satterthwaite-approximated degrees of freedom. Pairwise comparisons were adjusted for multiple testing by Holm method.

Seventeen piglets were analyzed, with a median blood withdrawal of 38 [34; 42] $mL \cdot kg^{-1}$. Median carotid, femoral, renal and mesenteric TAMV values and their interquartile ranges were 16 [14; 20], 23 [15; 29], 26 [19; 42] and 55 [40; 66] $cm \cdot s^{-1}$ at T0; 19 [15; 24], 25 [19; 38], 25 [17; 30] and 44 [36; 53] $cm \cdot s^{-1}$ at 10 $mL \cdot kg^{-1}$; 17 [14; 24], 26 [22; 40], 26 [18; 34] and 41 [38; 48] $cm \cdot s^{-1}$ at 20 $mL \cdot kg^{-1}$; 21 [16; 22], 25 [19; 32], 23 [19; 31] and 41 [36; 51] $cm \cdot s^{-1}$ at 30 $mL \cdot kg^{-1}$; and 20 [17; 22], 27 [25; 30], 16 [14; 16] and 48 [39; 59] $cm \cdot s^{-1}$ at 40 $mL \cdot kg^{-1}$, respectively. Overall territorial comparisons were F (3, 109) = 17.14 ($p < 0.01$) at T0 and F (3, 109) = 18.92 ($p < 0.01$) at T1. Within-territory analyses were F (8, 93) = 1.69 (Holm-adjusted p = 0.34) for the carotid territory, F (8, 91) = 2.10 (Holm-adjusted p = 0.18) for the femoral territory, F (8, 76) = 1.02 (Holm-adjusted p = 0.43) for the mesenteric territory, and F (8, 96) = 1.55 (Holm-adjusted p = 0.34) for the renal territory. The depletion step-by-territory interaction was F (24, 393) = 0.85 (p = 0.68).

The variations in RBF assessed by Doppler appeared to be heterogeneous across different territories, with carotid blood flow remaining preserved, although the study's statistical power was insufficient to confirm this difference.

Introduction

Hemorrhage remains a major cause of early and potentially preventable death after severe trauma, with a substantial proportion of deaths occurring before hospital admission [1,2]. Hemorrhagic shock results from acute blood loss leading to reduced venous return, stroke volume, cardiac output, oxygen delivery and tissue perfusion [3,4]. In response to hypovolemia, sympathetic activation and the release of endogenous vasoconstrictors aim to preserve arterial pressure and perfusion of vital organs [4,5]. These compensatory mechanisms induce heterogeneous regional vascular responses, including vasoconstriction of the renal, splanchnic and peripheral vascular beds [5–7]. Consequently, systemic

hemodynamic variables such as arterial pressure and cardiac output may not fully reflect the specific hemodynamic response of individual vascular territories [7,8].

Measuring the velocity-time integral (VTI) using Doppler ultrasound is a noninvasive and accessible method for assessing blood flow [9]. The VTI corresponds to the area under the Doppler velocity curve and represents the distance travelled by blood during one cardiac cycle, expressed in centimeters [9,10]. When the VTI is measured over a complete cardiac cycle, dividing it by the RR interval yields the time-averaged mean velocity (TAMV) according to the following equation TAMV = VTI / RR = VTI × heart rate (HR) / 60 [11–13]. Expressed in $cm \cdot s^{-1}$, the TAMV indicates the Doppler velocity per unit of time rather than the distance travelled per heartbeat, thereby accounting for concomitant variations in HR [13]. TAMV is used in vascular physiology to assess regional hemodynamics and blood flow in several arterial territories, including the carotid, vertebral, femoral and brachial arteries [14–18]. Combined assessment of multiple vascular territories has shown that their regional blood flow (RBF) may differ under various physiological conditions [15–18]. However, RBF and TAMV changes during progressive hemorrhage remain poorly documented, particularly in the carotid, femoral, renal and superior mesenteric arteries.

The porcine model is a preclinical model allowing for detailed study of changes in perfusion in different vascular territories, with the possibility of combining ultrasound measurements with invasive and laboratory data [19]. Several studies have suggested that carotid blood flow may remain relatively preserved during hemorrhagic shock [19,20].

The hypothesis of the study was that, during hemorrhagic shock, RBF rates assessed by TAMV would decrease differently during blood volume depletion.

The primary objective was to describe changes in TAMV among the carotid, femoral, superior mesenteric and renal arterial territories across blood depletion during controlled hemorrhagic shock in anesthetized piglets.

Methods

Study Type and Agreements

This experimental study was conducted using a controlled hemorrhagic shock model in piglets previously used and published by the research team (Coisy et al. Sci Rep 2025). The Languedoc-Roussillon Committee for the Protection and Use of Animals (9341-2021012709128801) approved the protocol, and all experiments were performed in an accredited animal research laboratory (RAM-PTNIM, Montpellier University, Medical School of Nimes, France). This study was conducted in accordance with European Directive 2010/63/EC and the recommendations governing the use of animals in scientific research. All facilities and means of transport complied with current legal requirements. This study is reported in accordance with the ARRIVE 2.0 guidelines.

Animal preparation and instrumentation

The piglets were Large White of 2–3 months of age, reared in an appropriate farm (Gaec Maruejols Le Bès, Sauveterre de rouergue, France). Eighteen piglets aged three to four months were included in the study. As previously described, the animals received premedication consisting of an intramuscular injection of 10 $mg{\cdot}kg^{-1}$ ketamine and 1 $mg{\cdot}kg^{-1}$ midazolam. Anesthesia was induced by administering a bolus of 4 $mg{\cdot}kg^{-1}$ propofol intravenously into a peripheral vein in the ear. Anesthesia was maintained by administering propofol at a rate of 8 $mg{\cdot}kg^{-1}{\cdot}h^{-1}$. The piglets were ventilated following orotracheal intubation using a ventilator (Aestiva 3000®; GE Healthcare; Madison; WI; USA) with an inspired oxygen fraction adjusted for the first arterial blood sample, at a tidal volume of 8 $mg{\cdot}kg^{-1}$ and a positive end-expiratory pressure of 5 cmH_2O. Once the piglets were anesthetized, a 7-Fr triple-lumen catheter was inserted under ultrasound guidance via the internal jugular vein. The central venous line was used to monitor central venous pressure and to inject boluses of cold water as part of transpulmonary thermodilution. A 5-Fr arterial catheter equipped with an integrated thermistor tip was inserted via a femoral artery (PiCCO Plus; Pulsion Medical Systems; Munich; Germany) to continuously monitor arterial pressure and collect arterial blood samples. The side of insertion for the arterial catheter was randomized as part of a separate protocol. A 20-gauge arterial catheter was inserted via the contralateral femoral artery (QuickFlash®; Teleflex; Morrisville; NC; USA). An 8.5 Fr catheter (Arrow; Arrow International; Inc.; Cleveland; OH; USA) was also placed in a femoral vein or a jugular vein for blood sampling and the administration of resuscitation fluids. All pressure measurement catheters were connected to transducers (PiCCO Plus) to continuously record systemic arterial pressure and HR.

Experimental protocol and measurement times

Briefly, T0 indicates the start of the experiment, with the mean arterial pressure (MAP) measured at this point serving as the baseline value. Blood depletion was then initiated in 2.5-minute increments via the 8.5-Fr venous catheter at a flow rate of 2 $mL{\cdot}kg^{-1}{\cdot}min^{-1}$ until a MAP of 40 mmHg was achieved, defining time T1. After T1, MAP was maintained between 35 and 45 mmHg for 30 minutes (T2). Subsequent resuscitation phases (T2a to T4) were conducted for other experimental purposes and were not included in the present analysis. All animals were euthanized at the end of the protocol with 2 g of thiopental. All steps are shown in Supplementary Fig. 1.

Several measurements were taken at the T0 phase: hemodynamic parameters (systolic and diastolic blood pressure, MAP, HR, cardiac output), arterial biochemical parameters (lactate, blood gases), and echocardiographic parameters (carotid, femoral, renal and superior mesenteric VTI). All echocardiographic parameters were recorded on the right side of the piglet. Hemodynamic and echocardiographic parameters were recorded at all blood depletion levels of 5 $mL{\cdot}kg^{-1}$ (T0a, T0b, T0c… up to T1). All parameters were recorded at T1. Additional measurements obtained during the subsequent maintenance and resuscitation phases (T1a to T4) were collected for other experimental purposes and were not included in the present analysis.

Vascular Doppler ultrasound

Vascular Doppler ultrasound was performed using a Versana Balance system (Versana Balance ; GE Medical Systems ; Milwaukee ; WI ; USA) equipped with a convex transducer (GE 4C-RS convex array probe ; GE Medical Systems ; Milwaukee ; WI ; USA) and a linear transducer (GE L6-12-RS linear array probe ; GE Medical Systems ; Milwaukee ; WI ; USA). The carotid VTI and femoral VTI were measured with the linear transducer, and the mesenteric VTI and renal VTI with the convex transducer. All VTI were calculated by averaging three measurements. An ultrasound registration was performed before the start of each protocol to identify the optimal ultrasound views for VTI measurement. Ultrasound examinations were systematically performed in the following order: carotid, femoral, superior mesenteric and renal territories. Regional TAMV values were calculated from VTI and HR using the following equation: TAMV = VTI × HR / 60. All archived ultrasound images were analyzed offline by a single investigator using EchoPAC Software-only (version 206.44.0; GE Healthcare). VTI contours were traced manually, without using the ultrasound system's automated tracing function, and TAMV was subsequently calculated offline rather than generated by integrated ultrasound software. No preferred side was specified for carotid and femoral ultrasound examinations, whereas all renal examinations were performed on the right kidney. All ultrasound acquisitions were performed by the same operator.

Objectives and outcomes

The primary objective was to describe the evolution of RBF, assessed using TAMV, in the carotid, femoral, superior mesenteric and renal arterial territories across blood depletion in anesthetized piglets. The primary outcome was the evolution of TAMV at every 5 mL.kg-1 blood-depletion steps, presented as individual trajectories normalized to baseline.

The first secondary objective was to compare TAMV among the four arterial territories before hemorrhage at T0 and at the end of blood depletion at T1, using an overall comparison followed by pairwise comparisons. The corresponding outcome was raw TAMV, expressed in $cm \cdot s^{-1}$, measured in each arterial territory at T0 and T1. The second secondary objective was to assess changes in TAMV across blood-depletion steps within each arterial territory. The corresponding outcome was TAMV normalized to its respective value at T0, with T0 defined as 1, across blood-depletion steps within each territory. The third secondary objective was to compare the evolution of TAMV across blood depletion among arterial territories. The corresponding outcome was the depletion step-by-territory interaction for TAMV normalized to T0 in the linear mixed-effects model.

Statistical analysis

The number of subjects required to detect a minimum 25% decrease in TAMV values compared with baseline during the hemorrhagic phase was estimated assuming a standard deviation of 0.25, an intra-subject correlation coefficient of 0.6 and a minimum of 5 measurements (T0 to T1). A total of 15 piglets was required to achieve 80% statistical power with a two-sided alpha risk of 5%. To account for potential

data loss (exclusions, unusable measurements, complications) estimated at 20%, the total number of animals to be included was increased to 18 piglets. Statistical analyses were performed using the R software (R Foundation for Statistical Computing, Vienna, Austria). Quantitative variables were described by their median and interquartile range [25th–75th percentiles], and qualitative variables by their frequencies and percentages. Statistical analyses were performed using all available observations and subjects with missing values were excluded only from the corresponding analysis. PiCCO-derived cardiac output was included as a descriptive hemodynamic reference but was not included in the inferential analyses. Missing data were not imputed.

For the primary outcome, TAMV values were normalized to each subject's baseline value, with T0 defined as 1, and their distribution across blood-depletion steps was described using medians and interquartile ranges.

For the first secondary objective, raw TAMV values were compared among the four arterial territories at T0 and T1 using a linear mixed-effects model including time, arterial territory and their interaction as fixed effects, with a subject-specific random intercept. Overall territorial comparisons were performed separately at T0 and T1 using type III ANOVA with the Satterthwaite approximation for degrees of freedom. Pairwise comparisons among territories were subsequently performed at each time point using Tukey-adjusted p-values and 95% confidence intervals [21,22].

For the second secondary objective, TAMV values were normalized to baseline, with T0 defined as 1, and changes across blood-depletion steps were assessed separately within each arterial territory using linear mixed-effects models including depletion step as a categorical fixed effect and a subject-specific random intercept. Global effects were assessed using type III ANOVA with the Satterthwaite approximation, and p-values were adjusted across the four territories using the Holm method.

For the third secondary objective, TAMV values were normalized to baseline, with T0 defined as 1, and differences in their evolution among arterial territories were assessed using a linear mixed-effects model including depletion step, arterial territory and their interaction as fixed effects and a subject-specific random intercept. The interaction was assessed using type III ANOVA with the Satterthwaite approximation for degrees of freedom.

Role of the funding source

The funder of the study had no role in the study design, data collection, data analysis, data interpretation, or writing of the report.

Results

Population

Seventeen out of eighteen piglets (94%) with a balanced sex ratio and a median weight of 32 kg [32 ; 35] were included for primary and secondary objectives analysis as 1 (6%) piglet died before echography recording. Hemodynamic and laboratory parameters at T0 are presented in Table 1. The median volume of blood withdrawal was 38 [34; 42] $mL \cdot kg^{-1}$.

Table 1
Hemodynamic and biological characteristics at T0. *Values are presented as median and [Q1; Q3] = [25th percentile; 75th percentile].*

Variable	**Total (n = 17)**
Sex, n (%) Female	8 (47%)
Weight (kg) Median [Q1; Q3]	32.3 [31.7; 34.9]
Systolic arterial pressure (mmHg) Median [Q1; Q3]	93 [84; 106]
Mean arterial pressure (mmHg) Median [Q1; Q3]	76 [68; 82]
Diastolic arterial pressure (mmHg) Median [Q1; Q3]	62 [55; 67]
Heart rate (bpm) Median [Q1; Q3]	105 [82; 115]
Cardiac output measured by PiCCO ($L \cdot min^{-1}$) Median [Q1; Q3]	2.2 [1.8; 3.2]
Arterial lactate ($mmol \cdot L^{-1}$) Median [Q1; Q3]	0.42 [0.26; 0.50]

Primary objective: changes in RBF

Regional TAMV values across blood-depletion steps are presented in Table 2. The spaghetti plot included 117 (99%) carotid, 113 (96%) femoral, 97 (82%) mesenteric and 117 (99%) renal observations. The boxplots included 117 (99%) carotid, 113 (96%) femoral, 110 (93%) mesenteric and 117 (99%) renal measurements. Changes in carotid, femoral, superior mesenteric and renal TAMV, together with PiCCO-derived cardiac output are presented in Fig. 1.A. Raw TAMV and cardiac output distributions across blood-depletion steps are presented as boxplots in Fig. 1.B.

Table 2

Regional blood flow assessed using time-averaged mean velocity across blood-depletion steps. Values are presented as median and [Q1; Q3] = [25th percentile; 75th percentile]. TAMV = time-averaged mean velocity and is expressed in cm·s⁻¹. Blood-depletion volume is expressed in mL·kg⁻¹.

Depletion steps (mL·kg⁻¹)	Carotid TAMV (cm·s⁻¹)	Femoral TAMV (cm·s⁻¹)	Mesenteric TAMV (cm·s⁻¹)	Renal TAMV (cm·s⁻¹)
0	16 [14; 20]	23 [15; 29]	55 [40; 66]	26 [19; 42]
5	19 [12; 25]	28 [16; 41]	52 [38; 64]	25 [20; 34]
10	19 [15; 24]	25 [19; 38]	44 [36; 53]	25 [17; 30]
15	23 [15; 29]	32 [20; 40]	51 [41; 69]	27 [19; 36]
20	17 [14; 24]	26 [22; 40]	41 [38; 48]	26 [18; 34]
25	21 [19; 25]	28 [21; 47]	41 [33; 52]	22 [18; 32]
30	21 [16; 22]	25 [19; 32]	41 [36; 51]	23 [19; 31]
35	18 [15; 22]	24 [22; 26]	35 [31; 55]	19 [17; 27]
40	20 [17; 22]	27 [25; 30]	48 [39; 59]	16 [14; 16]

Secondary objectives: Comparison of RBF rates

A total of 133 (98%) TAMV observations were analyzed for comparisons among arterial territories at T0 and T1, including 66 (97%) measurements at T0 and 67 (99%) at T1, with overall and pairwise comparisons presented in Table 3 and Table 4, respectively.

Table 3

Overall comparisons of time-averaged mean velocity among arterial territories at T0 and T1. Values are presented as median and [Q1; Q3] = [25th percentile; 75th percentile]. Values were obtained from a linear mixed-effects model including time, arterial territory and their interaction, with a subject-specific random intercept. CI = confidence interval; df = degrees of freedom; T0 = baseline; T1 = end of blood depletion.

Time	Carotid TAMV (cm·s⁻¹)	Femoral TAMV (cm·s⁻¹)	Renal TAMV (cm·s⁻¹)	Mesenteric TAMV (cm·s⁻¹)	*F* (numerator df, denominator df)	p-value
T0	16 [14; 20]	23 [15; 29]	55 [40; 66]	26 [19; 42]	17.14 (3, 109)	< 0.01
T1	17 [14; 22]	23 [16; 27]	51 [37; 59]	17 [13; 21]	18.92 (3, 109)	< 0.01

Table 4

Pairwise comparisons of time-averaged mean velocity among arterial territories at T0 and T1. Values are presented as median and [Q1; Q3] = [25th percentile; 75th percentile]. Values were obtained from a linear mixed-effects model including time, arterial territory and their interaction, with a subject-specific random intercept. Pairwise comparisons were adjusted using the Tukey method. Estimated differences were calculated as the first territory minus the second. CI = confidence interval; df = degrees of freedom; T0 = baseline; T1 = end of blood depletion.

Comparison	Time	Estimated difference [95% CI] in $cm \cdot s^{-1}$	Adjusted p-value
Carotid – femoral	T0	− 12 [− 25; 1]	0.08
Carotid - Mesenteric	T0	− 37 [− 50; − 23]	< 0.01
Carotid - Renal	T0	− 12 [− 25; 1]	0.07
Femoral - Mesenteric	T0	− 24 [− 38; − 11]	< 0.01
Femoral - Renal	T0	0 [− 13; 13]	0.99
Mesenteric - Renal	T0	24 [11; 38]	< 0.01
Carotid - Femoral	T1	− 3 [− 17; 10]	0.92
Carotid - Mesenteric	T1	− 32 [− 45; − 19]	< 0.01
Carotid - Renal	T1	− 1 [− 14; 12]	0.99
Femoral - Mesenteric	T1	− 29 [− 42; − 16]	< 0.01
Femoral - Renal	T1	3 [− 11; 16]	0.96
Mesenteric - Renal	T1	31 [18; 44]	< 0.01

Type III ANOVA showed F (8, 93) = 1.69 (Holm-adjusted p = 0.34) for the carotid territory, F (8, 91) = 2.10 (Holm-adjusted p = 0.18) for the femoral territory, F (8, 76) = 1.02 (Holm-adjusted p = 0.43) for the mesenteric territory, and F (8, 96) = 1.55 (Holm-adjusted p = 0.34) for the renal territory. Regional TAMV values across blood-depletion steps are presented in Table 2. The depletion step-by-territory interaction was F (24, 393) = 0.85 (p = 0.68).

Discussion

RBF across arterial territories during progressive blood depletion showed an heterogenous pattern, as assessed using Doppler-derived TAMV. After normalization to baseline, carotid RBF appeared relatively preserved throughout the hemorrhagic phase and appeared higher than the other regional trajectories. Femoral RBF showed an intermediate pattern, with an initial increase followed by lower values at the highest depletion steps, whereas renal and mesenteric TAMV were generally below baseline. TAMV levels differed among territories, whereas no within-territory changes or between-territory differences in TAMV trajectories were identified during progressive blood depletion.

The apparent preservation of carotid RBF during blood depletion, as assessed using TAMV, is consistent with preservation of the carotid velocity signal during hemorrhage [23]. This result may reflect compensatory centralization of the circulation toward organs considered essential for immediate survival, particularly the heart and brain, through sympathetic vasoconstriction in less immediately vital vascular beds [3–5]. The analysis did not identify a depletion step-by-territory interaction. The discrepancy between the graphical pattern in Fig. 2 and the interaction test may be related to insufficient statistical power.

Raw mesenteric TAMV was higher than carotid, femoral and renal TAMV both before hemorrhage at T0 and at the end of blood depletion at T1. Because this pattern was already present before hemorrhage and persisted at T1, it is more likely to reflect intrinsic hemodynamic, anatomical or technical differences among arterial territories than a response specifically induced by blood depletion. Experimental studies have nevertheless demonstrated reductions in mesenteric blood flow and vascular volume during hemorrhage, reflecting recruitment of the splanchnic blood reservoir and increased regional vascular resistance [5,7]. The higher mesenteric TAMV observed in the present study should not be considered contradictory to these findings because Doppler velocity is determined by the combined effects of volumetric flow and arterial cross-sectional area [9,24,25]. Mesenteric arterial flow also exhibits specific characteristics, including a high-resistance Doppler profile and substantial variability related to vascular compliance and acquisition conditions [26]. Whereas the aorta is an elastic artery, the superior mesenteric artery is predominantly muscular and has distinct compliance and flow-damping properties that may influence its Doppler velocity profile [27,28]. Mesenteric Doppler assessment is also technically challenging and operator dependent. In piglets, the proximal segment near the aortic origin may be more accessible than distal portions of the vessel, and inadvertent partial sampling of aortic velocities may have contributed to some high or outlying measurements. These anatomical and technical constraints may also explain the inter-individual variability and lower number of available mesenteric observations. Although the within-territory analysis did not identify changes in mesenteric TAMV normalized to baseline across blood-depletion steps, this finding should not be interpreted as evidence of preserved mesenteric perfusion. Higher raw mesenteric TAMV at T0 and T1 does not indicate greater volumetric blood flow, and an unchanged Doppler velocity may coexist with reduced blood flow when arterial cross-sectional area changes [24,25].

We did not identify changes in TAMV normalized to baseline across blood-depletion steps within any of the four arterial territories. This result contrasts with the reductions in renal and splanchnic blood flow previously described during hemorrhage [5–7]. Renal hypoperfusion activates the renin–angiotensin system, increasing angiotensin II concentrations, renal vasoconstriction and renal vascular resistance [29]. Hemorrhage also reduces mesenteric blood flow and vascular volume through increased regional resistance and recruitment of the splanchnic blood reservoir [7]. However, a reduction in volumetric blood flow does not necessarily produce a proportional reduction in Doppler velocity because vasoconstriction may decrease arterial cross-sectional area and maintain velocity [27]. The absence of changes in normalized TAMV therefore does not exclude modifications in regional volumetric blood flow or tissue

perfusion. Inter-individual variability and the lower number of mesenteric observations compared with the other arterial territories may also have reduced the ability to identify within-territory changes.

The use of TAMV to assess RBF rather than VTI represents an important methodological feature of this study. VTI expresses the distance travelled during a cardiac cycle, whereas the product of VTI and HR represents the distance travelled per minute [10]. Parameters incorporating VTI and HR have been reported to improve the interpretation of Doppler measurements compared with VTI alone, particularly when HR varies [10,30]. Because tachycardia is a major compensatory response during hemorrhage, the conversion of VTI into TAMV reduced the dependence of the analyzed parameter on the duration and number of cardiac cycles [30]. TAMV has also been used to characterize vascular responses in several arterial territories and under different physiological interventions, supporting its use as a dynamic vascular parameter [14–18]. TAMV also have established clinical applications. In children with sickle cell disease, transcranial Doppler monitoring uses the TAMV as a reference parameter for stroke-risk stratification, illustrating the clinical relevance and potential value of TAMV [31]. In this study, raw and baseline-normalized TAMV values addressed two different questions. Raw TAMV, expressed in $cm \cdot s^{-1}$, was used to compare absolute velocity levels among arterial territories at T0 and T1. Baseline-normalized TAMV was used to assess the evolution of each territory relative to its own initial value, with T0 defined as 1. Consequently, carotid TAMV could appear relatively preserved during blood depletion even though mesenteric TAMV remained higher in absolute terms.

This study has several strengths. Blood depletion was controlled and quantified, allowing repeated measurements to be obtained across standardized hemorrhagic steps. Four arterial territories with distinct physiological functions were assessed within the same animals, thereby limiting the effect of between-subject variability. Ultrasound measurements were combined with invasive arterial monitoring and transpulmonary thermodilution in a previously characterized porcine model of hemorrhagic shock [19,32–35]. All examinations were performed by the same operator and according to a predefined acquisition sequence, reducing variability related to differences between operators.

Limitations

The sample was small and included only young, initially healthy anesthetized piglets, limiting extrapolation to human trauma patients with variable age, comorbidities, tissue injury and uncontrolled bleeding. Anesthesia and mechanical ventilation may modify autonomic responses, venous return and vascular tone and therefore influence both systemic and regional hemodynamics. Missing measurements were unevenly distributed across territories, with lower completeness for the mesenteric artery, and may have reduced the precision of the longitudinal comparisons. Measurements were performed by a single operator, and interobserver and intraobserver reproducibility were not evaluated. The fixed sequence of vascular examinations may also have introduced a temporal offset between territories during active blood withdrawal. Baseline normalization removed physiologically relevant differences in absolute velocity and may have amplified variability when baseline values were low.

Conclusion

In our study of a controlled, ventilated hemorrhagic shock model, the variations in RBF assessed by Doppler appeared to be heterogeneous across different territories, with carotid blood flow remaining preserved, although the study's statistical power was insufficient to confirm this difference.

Declarations

Acknowledgments

The authors thank Marylène Peltier for her help in administrative, technical, and logistical support, as well as Marc Giet and Jack Fountain for their help in animal preparation and for their technical assistance.

Author contributions

C.A. had full access to all the data in the study and takes responsibility for the integrity of the data and the accuracy of the data analysis.

Study concept and design: X.B, F.C., C.O., T.M., F.A., *Acquisition of data:* C.A., *Analysis and interpretation of data:* All authors, *Drafting of the manuscript:* All authors, *Critical revision of the manuscript for important intellectual content:* All authors, *Statistical analysis:* C.A., *Obtaining funding:* X.B., F.C., *Administrative, technical, or material support:* All authors, *Supervision:* X.B., F.C., C.O., T.M.

Funding

This study was funded by Nîmes university hospital and Montpellier University.

Competing interests

CA declares a conflict of interest for this study with Agence régionale de santé Occitanie, as he received a one-year research fellowship funded by Agence régionale de santé Occitanie. Other authors declare that they have no competing interests.

Data Availability Statement

The datasets generated and analyzed during the current study, including Doppler-derived TAMV measurements and hemodynamic data, are available from the corresponding author upon reasonable request.

References

1. Kauvar, D. S., Lefering, R. & Wade, C. E. Impact of hemorrhage on trauma outcome: an overview of epidemiology, clinical presentations, and therapeutic considerations. *J. Trauma.* **60**, S3–11 (2006).

2. Teixeira, P. G. R. et al. Preventable or potentially preventable mortality at a mature trauma center. *J. Trauma.* **63**, 1338–1346 (2007). discussion 1346–1347.
3. Novy, E. & Levy, B. Choc hémorragique: aspects physiopathologiques et prise en charge hémodynamique. *Réanimation* 24, 406–412 (2015).
4. Gutierrez, G., Reines, H. D. & Wulf-Gutierrez, M. E. Clinical review: hemorrhagic shock. *Crit. Care*. **8**, 373–381 (2004).
5. Bond, R. F. & Johnson, G. Vascular adrenergic interactions during hemorrhagic shock. *Fed. Proc.* 44, 281–289 (1985).
6. Lauson, H. D., Bradley, S. E., Cournand, A. & Andrews, V. V. THE RENAL CIRCULATION IN SHOCK 1. *J. Clin. Invest.* **23**, 381–402 (1944).
7. Lintermans, J., Appel, A., Bloom, R., Mullins, G. & Guntheroth, W. Mesenteric blood flow and vascular volume in hemorrhagic shock. *Am. J. Physiol. -Leg Content*. **212**, 482–487 (1967).
8. Cecconi, M. et al. Consensus on circulatory shock and hemodynamic monitoring. Task force of the European Society of Intensive Care Medicine. *Intensive Care Med.* **40**, 1795–1815 (2014).
9. Mercado, P. et al. Transthoracic echocardiography: an accurate and precise method for estimating cardiac output in the critically ill patient. *Crit. Care*. **21**, 136 (2017).
10. Blanco, P. Rationale for using the velocity–time integral and the minute distance for assessing the stroke volume and cardiac output in point-of-care settings. *Ultrasound J.* **12**, 21 (2020).
11. Cho, I. J. et al. Deceleration time of left ventricular outflow tract flow as a simple surrogate marker for central haemodynamics at rest and as well as during exercise. *Eur. Heart J. Cardiovasc. Imaging*. **18**, 568–575 (2017).
12. Quigley, K. S. et al. Publication guidelines for human heart rate and heart rate variability studies in psychophysiology-Part 1: Physiological underpinnings and foundations of measurement. *Psychophysiology* **61**, e14604 (2024).
13. Hitomi, Y. et al. Hemodialysis vascular sound index as a diagnostic tool for vascular access stenosis: a prospective matched observational study. *BMC Nephrol.* **27**, 244 (2026).
14. Khan, M. A. et al. Measurement of cerebral blood flow using phase contrast magnetic resonance imaging and duplex ultrasonography. *J. Cereb. Blood Flow. Metab.* **37**, 541–549 (2017).
15. Rourke, A. J. et al. Acute ketone monoester ingestion lowers resting cerebral blood flow: a randomized cross-over trial. *J. Physiol.* **604**, 2525–2541 (2026).
16. Turner, R. et al. Cerebral blood flow regulation in hypobaric hypoxia: role of haemoconcentration. *J. Physiol.* **602**, 5643–5657 (2024).
17. Tomoto, T. et al. Cerebral blood flow and cerebrovascular resistance across the adult lifespan: A multimodality approach. *J. Cereb. Blood Flow. Metab.* **43**, 962–976 (2023).
18. Watanabe, K. et al. Heat-related changes in the velocity and kinetic energy of flowing blood influence the human heart's output during hyperthermia. *J. Physiol.* **602**, 2227–2251 (2024).

19. Grau-Mercier, L. et al. Can blood loss be assessed by echocardiography? An experimental study on a controlled hemorrhagic shock model in piglets. *J. Trauma. Acute Care Surg.* **92**, 924–930 (2022).
20. Benham, D. A. et al. Is cerebral perfusion maintained during full and partial resuscitative endovascular balloon occlusion of the aorta in hemorrhagic shock conditions? *J. Trauma. Acute Care Surg.* **91**, 40–46 (2021).
21. Satterthwaite, F. E. An Approximate Distribution of Estimates of Variance Components. *Biom Bull.* **2**, 110 (1946).
22. Tukey, J. W. Comparing Individual Means in the Analysis of Variance. *Biometrics* **5**, 99 (1949).
23. Kenny, J. É. S. et al. A wireless ultrasound patch detects mild-to-moderate central hypovolemia during lower body negative pressure. *J. Trauma. Acute Care Surg.* **93**, S35–S40 (2022).
24. Drieghe, B. et al. Assessment of renal artery stenosis: side-by-side comparison of angiography and duplex ultrasound with pressure gradient measurements. *Eur. Heart J.* **29**, 517–524 (2008).
25. Nylund, K. et al. EFSUMB Recommendations and Guidelines for Gastrointestinal Ultrasound. *Ultraschall Med.* **38**, 273–284 (2017).
26. Herzog, M. J. et al. Arterial stiffness and vascular aging: mechanisms, prevention, and therapy. *Signal. Transduct. Target. Ther.* **10**, 282 (2025).
27. Bude, R. O., Larson, R. G., Nichols, W. W. & Rubin, J. M. Stenosis of the main artery supplying an organ: effect of end-organ vascular resistance on the poststenotic peak systolic velocity in an in vitro hydraulic model at Doppler US. *Radiology* **212**, 79–87 (1999).
28. Michel, J. B., Lagrange, J., Regnault, V. & Lacolley, P. Conductance Artery Wall Layers and Their Respective Roles in the Clearance Functions. *Arterioscler. Thromb. Vasc Biol.* **42**, e253–e272 (2022).
29. Bekassy, Z., Lopatko Fagerström, I., Bader, M. & Karpman, D. Crosstalk between the renin-angiotensin, complement and kallikrein-kinin systems in inflammation. *Nat. Rev. Immunol.* **22**, 411–428 (2022).
30. Solinski, A. et al. Centile Curves for Velocity-Time Integral Times Heart Rate as a Function of Ventricular Length: The Use of Minute Distance Is Advantageous to Enhance Clinical Reliability in Children. *J. Am. Soc. Echocardiogr*. **31**, 105–112e2 (2018).
31. Haute Autorité de Santé. *Syndromes drépanocytaires majeurs de l'enfant et de l'adolescent* (Haute Autorité de Santé, 2024).
32. Bobbia, X. et al. A New Echocardiographic Tool for Cardiac Output Evaluation: An Experimental Study. *Shock* **52**, 449–455 (2019).
33. Markarian, T. et al. Evaluation of a New Echocardiographic Tool for Cardiac Output Monitoring: An Experimental Study on A Controlled Hemorrhagic Shock Model in Anesthetized Piglets. *J. Clin. Med.* **11**, 5420 (2022).
34. Sanchez, T. et al. Is the shock index correlated with blood loss? An experimental study on a controlled hemorrhagic shock model in piglets. *Am. J. Emerg. Med.* **75**, 59–64 (2024).

35. Ajavon, F. et al. ARTERIAL DIAMETER VARIATIONS VOLUME ASSESSMENT: AN EXPERIMENTAL STUDY ON A CONTROLLED HEMORRHAGIC SHOCK MODEL IN PIGLETS. *Shock* 59, 637–645 (2023).

Figures

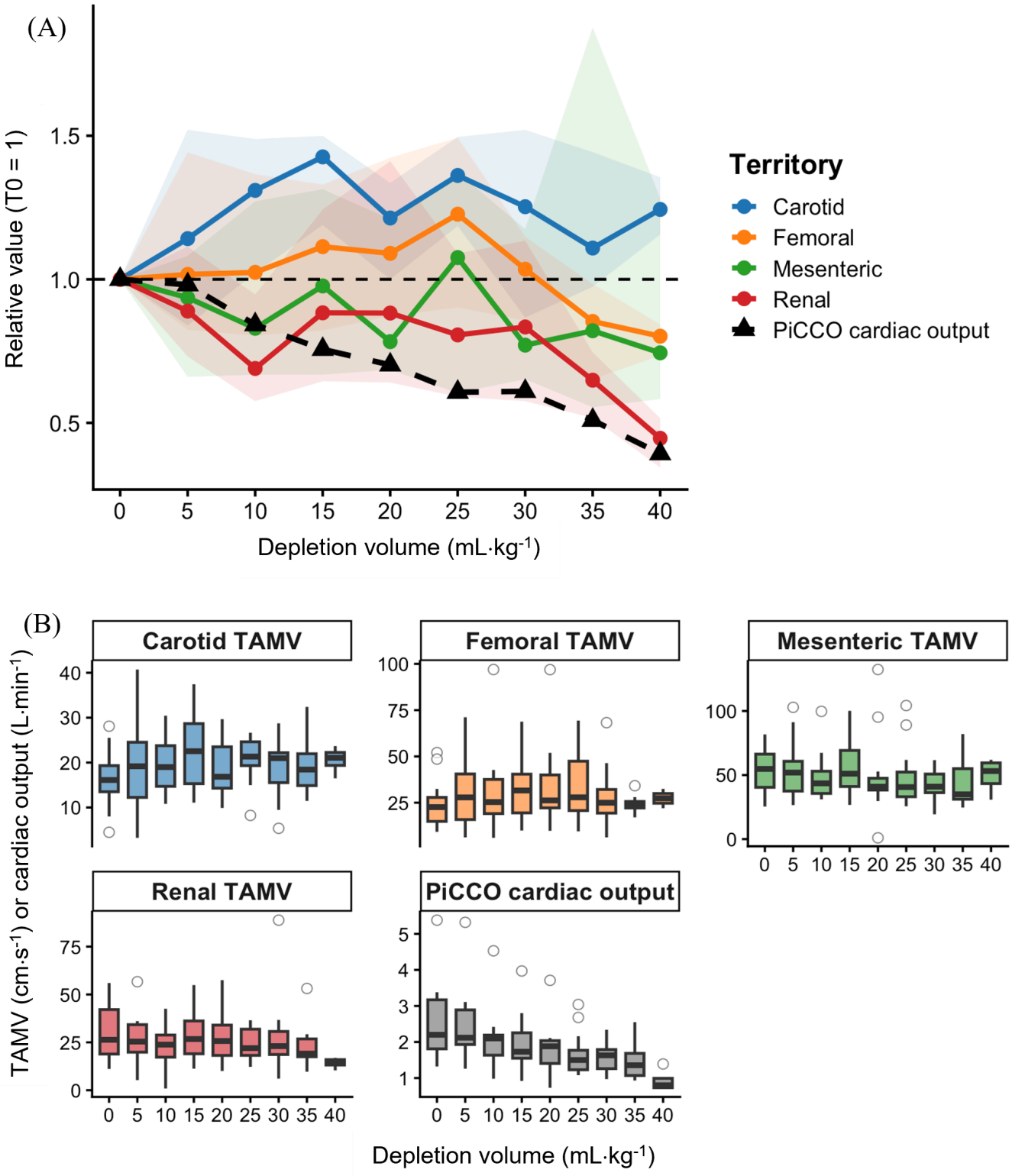


Figure 1

Regional blood flow assessed using time-averaged mean velocity (TAMV) and PiCCO-derived cardiac output during blood depletion. (A) Baseline-normalized values (T0 = 1), presented as medians and interquartile ranges. *Points and lines represent medians, shaded areas represent interquartile ranges, and the horizontal dashed line indicates the baseline reference value.* (B) Raw-value distributions presented as boxplots. *Boxes represent interquartile ranges, horizontal lines within boxes represent medians, and whiskers extend to the most extreme values within 1.5 times the interquartile range. TAMV is expressed in cm·s⁻¹ and PiCCO-derived cardiac output in L·min⁻¹. Separate vertical scales are used for each panel in (B).*

Supplementary Files

This is a list of supplementary files associated with this preprint. Click to download.

- SupplementaryFig.docx